J Mar Sci Technol (2008) 13:147–153
DOI 10.1007/s00773-007-0263-8

ORIGINAL ARTICLE

Mooring cable tracking using active vision for a biomimetic autonomous underwater vehicle

Jenhwa Guo

Received: June 7, 2007 / Accepted: November 7, 2007

Abstract This study presents a localization system using visual information for guidance and navigation of a biomimetic autonomous underwater vehicle (BAUV). The BAUV tracks a mooring cable using two cameras and sonar. Sonar has good accuracy in detecting longitudinal distances but is poor in detecting lateral distances. Since a stereo image has quantization errors, for the cameras, measurement errors in lateral directions are less than those in the optic-axis direction. An extended Kalman filter was employed to combine observational information derived from the cameras and sonar of the mooring cable position with the navigation data of the BAUV. This work demonstrates, using water tank experiments, the effectiveness of the proposed tracking technique in decreasing uncertainty in position estimations of the BAUV and mooring cable.

Key words Estimation · Visual motion · Kalman filter · Control · AUV

1 Introduction

Considerable effort within the oceanographic community has been devoted to developing underwater observational systems (Howe et al.[1]). To facilitate water column sampling in the ocean, a fixed mooring system with communication capabilities and a power coupler are typically utilized. Undersea vehicles, such as autonomous underwater vehicles (AUVs), have become important tools in undersea inspection and surveying. These AUVs dock to a mooring system to charge onboard batteries and exchange data; these are essential techniques for the operation of underwater observatories. Mooring cables also function as navigational landmarks for AUVs to locate their position while working around a mooring station. This study presents a technique for positional tracking of a mooring cable using a biomimetic AUV (BAUV). The low propulsive efficiency and poor maneuverability of conventional AUVs while hovering remain challenges for AUV designers. BAUVs mimic fish and have an excellent ability to perform precise hovering and agile turning; they have therefore received considerable attention from the research community. The design of the BAUV in this study is based on a fish motion model and has sensing, behavior planning, and motion control abilities. Sonar and two video cameras are installed on the head of the BAUV to detect environmental objects. Figure 1 presents the shape of the BAUV. The approach used for guiding the vehicle to an underwater docking station using mooring cable tracking first estimates the station location using sonar, and the BAUV then proceeds to a location within visible range of the mooring cable. A visual guidance mode is then activated to reach the mooring cable with good precision. Doppler sonar is typically utilized as velocity sensors for AUV guidance and navigation. Positional uncertainties derived from Doppler sonar increase over time. Positional information of underwater features observed by BAUV visual sensors reduces the positional uncertainty of a BAUV and increases the estimated precision of the mooring cable position.

In previous work, an optimal body spline allowing a BAUV to swim forward was identified by optimizing

J. Guo
Department of Engineering Science and Ocean Engineering, National Taiwan University, No. 1 Roosevelt Rd., Sec. 4, Taipei 106, Taiwan
e-mail: jguo@ntu.edu.tw

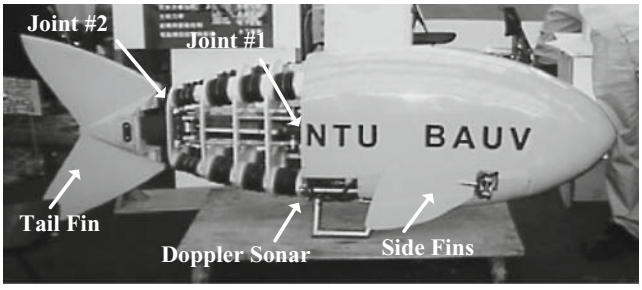

Fig. 1. Photograph of the biomimetic autonomous underwater vehicle (*BAUV*)

performance criteria using genetic algorithms (Guo et al.[2]). A waypoint tracking controller was designed that guides the BAUV (Guo[3]). Many successful robot-guidance schemes have been utilized for investigating visual tracking for navigation. Most schemes involve mobile robots and on-board mechanisms that control the viewing direction of visual sensors (Miura and Shirai,[4] Moon et al.,[5] Davison and Murray[6]). Guo et al.[7] proposed an on-line viewpoint and motion planning method for a BAUV to reach a target position under uncertainty. For submarine vehicles, Williams et al.[8] used a Kalman filter-based approach and feature extraction algorithms for localization and map generation. The feature extraction algorithm extracts appropriate features that are then utilized to create a map of the environment while simultaneously estimating vehicle location.

This study incorporates environmental observations with navigation data for estimation of the BAUV's position and the position of environmental features. A federated filter was utilized to combine estimated states and error covariances from sonar and binocular vision, respectively. The BAUV control system uses combined information as feedback for way-point control. The main contribution of this study is the proposed mooring station tracking algorithms for a fish-like underwater vehicle. An estimation and control method was devised for cable position tracking. This method was experimentally verified to enable a biomimetic underwater vehicle to find and to reach a mooring cable. The remainder of this article is organized as follows. In Sect. 2, mathematical models of motion and observation uncertainties are described, and the proposed data fusion approach utilizing observational information for updating states and their uncertainties is presented. The hardware arrangement is described in Sect. 3. Experiments conducted in a water tank for verification of the proposed tracking algorithms are also presented in Sect. 3. Finally, conclusions are given in Sect. 4.

2 Modeling

The vehicle state, $\mathbf{X} = [x \quad y \quad \psi]^T$, consists of the head position (x, y) of the BAUV and orientation ψ. Control inputs are denoted by input vector $\mathbf{U} = [u \quad \gamma]^T$, which comprises advancing velocity and angular velocity. Velocity u is controlled directly by the oscillating frequency and oscillating amplitude of the tail, whereas angular velocity γ is controlled by the body-spline offset parameter (Guo and Joeng[9]). The state transition of the BAUV can be expressed by the following nonlinear equation:

$$\mathbf{X}_{t+1} = \begin{bmatrix} x_t + (u_t \cos\psi_t - v_t \sin\psi_t)\cdot\Delta t \\ y_t + (u_t \sin\psi_t + v_t \cos\psi_t)\cdot\Delta t \\ \psi_t + \gamma_t \cdot \Delta t \end{bmatrix} = \mathbf{F}(\mathbf{X}_t, \mathbf{U}_t) \tag{1}$$

where $\mathbf{X}_{t+1}$ is the predicted state at time t; x_t, y_t, and ψ_t are positions and orientation of the BAUV at time t; u_t, v_t, *and* γ_t represent translational and rotational velocities of the BAUV; and Δt is the time interval. To predict the uncertainty of $\mathbf{X}_{t+1}$, Eq. 1 is linearized using the Taylor series expansion around mean values $\hat{\mathbf{X}}_t$ and $\hat{\mathbf{U}}_t$:

$$\mathbf{X}_{t+1} \approx \mathbf{F}(\hat{\mathbf{X}}_t, \hat{\mathbf{U}}_t) + \frac{\partial \mathbf{F}}{\partial \mathbf{X}_t}(\mathbf{X}_t - \hat{\mathbf{X}}_t) + \frac{\partial \mathbf{F}}{\partial \mathbf{U}_t}(\mathbf{U}_t - \hat{\mathbf{U}}_t) \tag{2}$$

The covariance matrix of the predicted state error covariance, $\Sigma_{X_{t+1}}$, can be obtained by:

$$\begin{aligned} \sum\nolimits_{X_{t+1}} &= E[(\mathbf{X}_{t+1} - \mathbf{X}_{t+1})(\mathbf{X}_{t+1} - \mathbf{X}_{t+1})^T] \\ &\cong \frac{\partial \mathbf{F}}{\partial \mathbf{X}_t} \sum\nolimits_{X_t} \frac{\partial \mathbf{F}^T}{\partial \mathbf{X}_t} + \frac{\partial \mathbf{F}}{\partial \mathbf{U}_t} \sum\nolimits_{U_t} \frac{\partial \mathbf{F}^T}{\partial \mathbf{U}_t} \end{aligned} \tag{3}$$

where E produces the expected values, Σ_U is the covariance matrix of the control input. Assuming that errors in the control vector are Gaussian and independent, the positional uncertainty of the BAUV can be illustrated by projecting the covariance matrix Σ_X into the horizontal plane.

For a mooring cable located at $\mathbf{L} = [L_x \quad L_y]^T$ in world coordinates, the observational equation can be expressed as:

$$\mathbf{L} = \mathbf{R}_{[\rho]}\mathbf{O} + \mathbf{X} \tag{4}$$

where $\mathbf{R}_{[\rho]}$ is the rotation matrix with angle ρ. Equation 4 is a constraint equation for the BAUV at state **x** that generates observation **O** of an unknown feature **L**. Figure 2 illustrates coordinates for the sensors and the target. Equation 4 can be rewritten as:

$$\mathbf{G}(\mathbf{X}, \mathbf{O}, \mathbf{L}) = \mathbf{L} - \mathbf{R}_{[\rho]}\mathbf{O} - \mathbf{X} = 0 \tag{5}$$

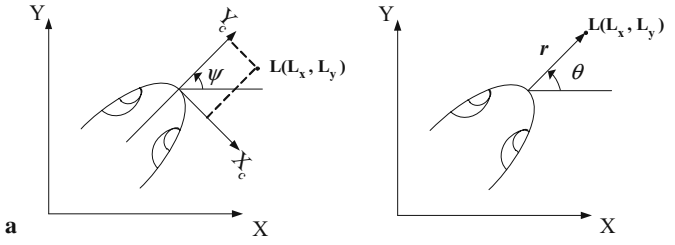

Fig. 2. Coordinate systems for the sensors and the target. **a** Camera, **b** sonar

Equation 5 can then be written into the following expressions for camera and sonar measurements. The observational equation for camera measurements is defined as:

$$\mathbf{G}(\mathbf{X}_t, \mathbf{O}_c, \mathbf{L}) = \mathbf{L} - \mathbf{R}_{\left[\psi-\frac{\pi}{2}\right]}\mathbf{O}_c - \mathbf{X}_t = 0$$

$$\mathbf{G}(\mathbf{X}_t, \mathbf{O}_c, \mathbf{L}) = \begin{bmatrix} L_x - \sin\psi \cdot O_{cx} - \cos\psi \cdot O_{cy} - x_t \\ L_y + \cos\psi \cdot O_{cx} - \sin\psi \cdot O_{cy} - y_t \end{bmatrix}$$

$$\mathbf{R}_{\left[\psi-\frac{\pi}{2}\right]} = \begin{bmatrix} \sin\psi & \cos\psi \\ -\cos\psi & \sin\psi \end{bmatrix}$$

$$\mathbf{O}_c = \mathbf{Z}(\mathbf{I}) = \begin{bmatrix} O_{cx} \\ O_{cy} \end{bmatrix} = \begin{bmatrix} \frac{x_l + x_r}{x_l - x_r} \cdot a \\ \frac{2f}{x_l - x_r} \cdot a \end{bmatrix}$$

where f and $2a$ are the camera focal length and the distance between the two cameras, respectively. Projected position $\mathbf{I} = [x_l \quad x_r]^T$ includes an error caused by image quantization. Errors x_l and x_r can be modeled as Gaussian errors and are independent (Miura and Shirai[4]). Conversely, the observational equation for sonar measurements can be represented as:

$$\mathbf{G}(\mathbf{X}_t, \mathbf{O}_s, \mathbf{L}) = \mathbf{L} - \mathbf{R}_{[0]}\mathbf{O}_s - \mathbf{X}_t = 0$$

$$\mathbf{G}(\mathbf{X}_t, \mathbf{O}_s, \mathbf{L}) = \begin{bmatrix} L_x - O_{sx} - x_t \\ L_y - O_{sy} - y_t \end{bmatrix}$$

$$\mathbf{O}_s(r, \theta) = \begin{bmatrix} r\cos\theta \\ r\sin\theta \end{bmatrix}$$

These equations are linearized using the Taylor series expansion around mean values $\hat{\mathbf{X}}$, $\hat{\mathbf{O}}$, and $\hat{\mathbf{L}}$:

$$\mathbf{G}(\mathbf{X}, \mathbf{O}, \mathbf{L}) \approx \mathbf{G}(\hat{\mathbf{X}}, \hat{\mathbf{O}}, \hat{\mathbf{L}}) + \frac{\partial \mathbf{G}}{\partial \mathbf{X}}(\mathbf{X} - \hat{\mathbf{X}}) + \frac{\partial \mathbf{G}}{\partial \mathbf{O}}(\mathbf{O} - \hat{\mathbf{O}}) + \frac{\partial \mathbf{G}}{\partial \mathbf{L}}(\mathbf{L} - \hat{\mathbf{L}}) = 0 \tag{6}$$

Equation 6 can be rewritten into the following linear equation:

$$\mathbf{Y} = \mathbf{H}\mathbf{X} + \mathbf{V} \tag{7}$$

where

$$\mathbf{Y} = -\mathbf{G}(\hat{\mathbf{X}}, \hat{\mathbf{O}}, \hat{\mathbf{L}}) + \frac{\partial \mathbf{G}}{\partial \mathbf{X}}\hat{\mathbf{X}}$$

$$\mathbf{H} = \frac{\partial \mathbf{G}}{\partial \mathbf{X}}$$

$$\mathbf{V} = \frac{\partial \mathbf{G}}{\partial \mathbf{O}}(\mathbf{O} - \hat{\mathbf{O}}) + \frac{\partial \mathbf{G}}{\partial \mathbf{L}}(\mathbf{L} - \hat{\mathbf{L}})$$

In Eq. 7, $\mathbf{Y}$ is a new observation, $\mathbf{H}$ is the linear transformation from $\mathbf{X}$ to $\mathbf{Y}$, and $\mathbf{V}$ is the observational error. The covariance matrix of observation Σ_V, which consists of observational uncertainty Σ_O and positional uncertainty of the mooring cable Σ_L, is expressed as

$$\sum\nolimits_V = E[\mathbf{V}\mathbf{V}^T] = \frac{\partial \mathbf{G}}{\partial \mathbf{O}}\sum\nolimits_O \frac{\partial \mathbf{G}^T}{\partial \mathbf{O}} + \frac{\partial \mathbf{G}}{\partial \mathbf{L}}\sum\nolimits_L \frac{\partial \mathbf{G}^T}{\partial \mathbf{L}} \tag{8}$$

We assume that the global position and the positional uncertainty of the docking station are known. Positional estimate $\hat{\mathbf{L}}$ is first estimated made by sonar. When the cable is in the cameras' visible range, view points of the BAUV can be planned thereafter using observational data acquired by the video cameras. Based on the observation and estimation of the cable location, the state and the uncertainty in the state of the BAUV can be estimated and updated using a Kalman filter, as expressed by the following equations:

$$\hat{\mathbf{X}}_t = \mathbf{F}(\bar{\mathbf{X}}_{t-1}, \mathbf{U}_{t-1})$$

$$\sum\nolimits_{\hat{X}_t} = \frac{\partial \mathbf{F}}{\partial \mathbf{X}_{t-1}}\sum\nolimits_{\bar{X}_{t-1}} \frac{\partial \mathbf{F}^T}{\partial \mathbf{X}_{t-1}} + \frac{\partial \mathbf{F}}{\partial \mathbf{U}_{t-1}}\sum\nolimits_{U_{t-1}} \frac{\partial \mathbf{F}^T}{\partial \mathbf{U}_{t-1}}$$

$$\mathbf{K} = \sum\nolimits_{\hat{X}_t} \mathbf{H}^T \left[\mathbf{H}\sum\nolimits_{\hat{X}_t} \mathbf{H}^T + \sum\nolimits_V\right]^{-1}$$

$$\sum\nolimits_{\bar{X}_t} = [\mathbf{I} - \mathbf{K}\mathbf{H}]\sum\nolimits_{\hat{X}_t}$$

$$\bar{\mathbf{X}}_t = \hat{\mathbf{X}}_t + \mathbf{K}[\mathbf{Y} - \mathbf{H}\hat{\mathbf{X}}_t] \tag{9}$$

where $\bar{\mathbf{X}}_t$ and $\Sigma_{\bar{X}_t}$ are the estimated state and covariance matrix, respectively; $\hat{\mathbf{X}}_t$ and $\Sigma_{\hat{X}_t}$ are the predicted state and covariance matrix, respectively; and $\mathbf{K}$ is the Kalman gain. The elements in Eq. 9 are derived separately for the cameras and sonar; in other words, each filter is dedicated to an individual sensor system. We assume that the estimation of each filter is independent. Given the outputs of a set of filters for the camera and sonar with state estimates $\bar{\mathbf{X}}_c$ and $\bar{\mathbf{X}}_s$, and their corresponding error covariances $\Sigma_{\bar{\mathbf{x}}_c}$ and $\Sigma_{\bar{\mathbf{x}}_s}$, following data fusion, the state

estimation is considered a linear combination from state estimates (Carlson[10]):

$$\sum = \left[\sum_{\bar{\mathbf{x}}_c}^{-1} + \sum_{\bar{\mathbf{x}}_s}^{-1}\right]^{-1}$$
$$\bar{\mathbf{X}} = \left[\sum_{\bar{\mathbf{x}}_c}^{-1} + \sum_{\bar{\mathbf{x}}_s}^{-1}\right]^{-1}\left(\sum_{\bar{\mathbf{x}}_c}^{-1}\bar{\mathbf{X}}_c + \sum_{\bar{\mathbf{x}}_s}^{-1}\bar{\mathbf{X}}_s\right) \quad (10)$$

3 Control

This section presents the control laws that control the BAUV when tracking a mooring cable. The control scheme first transfers body/caudal fin oscillations to the body-spline oscillations. A body-spline equation is utilized to represent the centre line of the BAUV body by continuously coordinating the joint angles such that they match the desired shape of the body spline in the BAUV body frame. Figure 3 presents a conceptual view of the body-spline shape. In Fig. 3, $y(x, t)$ is the body-spline equation, c_1 and c_2 are coefficients of the envelope, $k = 2\pi/\lambda$ is the body wave number, λ is the body wavelength, and f_c is the oscillation frequency. When the BAUV is turning, the parameter *offset* has a non-zero value. The body-spline equation representing the BAUV bodily motion is:

$$y(x,t) = (c_1 x + c_2 x^2)(A\sin(kx + 2\pi f_c t) + offset) \quad (11)$$

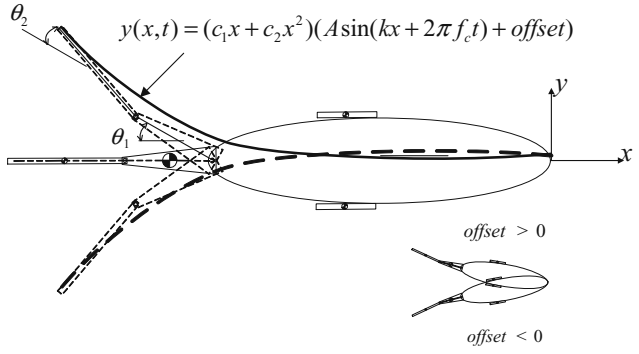

Fig. 3. BAUV body spline. c_1 and c_2 are coefficients of the envelope, A indicates the extent of tail movement, k is the body wave number, f_c is the oscillation frequency of the tail, and *offset* is non-zero if the BAUV is turning

According to (Guo et al.[2]), the BAUV body spline is obtained using coefficients $c_1 = -0.075$, $c_2 = 0.017$, and $\lambda = 3.6$. The operational ranges of parameter values are determined based on the angular limitations of the joint motors. The parameter *offset* determines the offset of the fish body spline while swimming. Variable A approaches 1 when using the full envelope of the caudal fins and A is reduced to zero when no caudal fin motion is required. The maximal swing of the body is set to $|offset| = 2$ and $A = 1$; θ_1, and θ_2 are joint motor positions determined by the body-spline equation.

The swimming behavior of the BAUV in relation to bodily motion was examined by experimentation using the free-run BAUV test bed. Swimming behavior curves demonstrate the relationship between A, f_c, *offset*, surge speed u, and yaw rate $\dot{\theta}_b$ of the BAUV (Fig. 4). The surge speed can be controlled by tuning A or f_c, and yaw rate can be modulated by tuning *offset*.

Figure 5 presents the overall feedback diagram for the control system. In Fig. 5, the target is the desired cable position in the global coordinate frame, θ^d is the desired global heading for the BAUV, and e is the heading error. The global controller provides commands to the body-spline controller and ensures that $\psi \to \theta^d$ based on state feedback. A proportional gain is employed for the global controller such that *offset* is proportional to heading error e. Filters 1 and 2 are Kalman filters for the sonar and the cameras, respectively. Estimates derived from Filters 1 and 2 are combined by a master filters, as in Eq. 10.

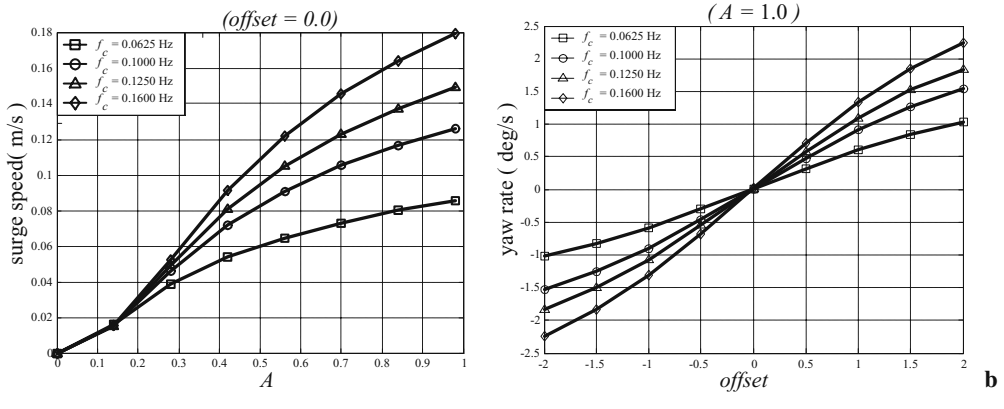

Fig. 4. Characteristics of the body/caudal fin plotted against surge speed and yaw rate. **a** Surge speed versus parameter A for various f_c values. **b** Yaw rate versus *offset* for various f_c values

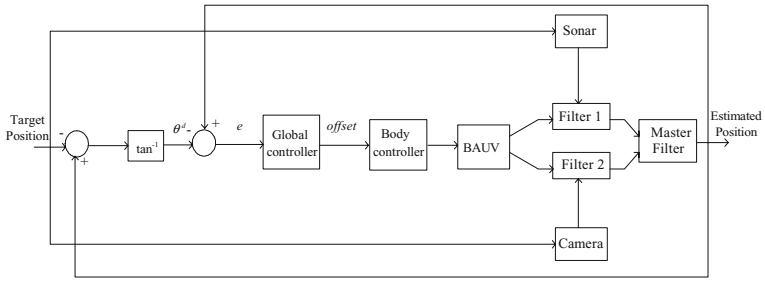

Fig. 5. Block diagram of the control system. θ^d is the desired global heading for the BAUV and e is the heading error

Experiments

In stereo imaging, the object distance is determined based on the disparity between two images captured using parallel cameras (Matthies and Shafer[11]). As the BAUV approaches the target, the disparity in the image plane does not reflect the real distance and involves errors. Since uncertainty increases with distance, it can be modeled using a weighting function whose magnitude is inversely related to object distance, i.e., a covariance matrix with structure $\mathbf{V}\mathbf{V}^T = w\mathbf{M}$, where w is a scalar and $\mathbf{M}$ is an identity matrix. Uncertainty caused by quantization error is:

$$\sum_o = \frac{\partial \mathbf{Z}}{\partial \mathbf{I}} w\mathbf{M} \frac{\partial \mathbf{Z}^T}{\partial \mathbf{I}} = \frac{4a^2}{(x_l - x_r)^4} \begin{bmatrix} x_r^2 + x_l^2 & x_r \cdot f + x_l \cdot f \\ x_r \cdot f + x_l \cdot f & 2f^2 \end{bmatrix} w \tag{12}$$

In Eq. 12, $\frac{\partial \mathbf{Z}}{\partial \mathbf{I}}$ is the matrix of the first partial derivatives of $\mathbf{O}$.

Uncertainties arise from the sonar because range readings produced by the system do not always correspond to objects at that range (Benet and Blanes[12]). Echo strength decreases as the range increases, and the relationship between sonar range and noise is modeled. A mathematical relationship between ranges and variances is established using a least-squares method; n pings were recorded for a target of known distance. Defining:

$$\mathbf{v}_0 = \begin{bmatrix} 1 \\ 1 \\ \vdots \\ 1 \end{bmatrix}, \quad \mathbf{v}_1 = \begin{bmatrix} x_1 \\ x_2 \\ \vdots \\ x_n \end{bmatrix}, \quad \mathbf{v}_2 = \begin{bmatrix} x_1^2 \\ x_2^2 \\ \vdots \\ x_n^2 \end{bmatrix}, \quad \text{and} \quad \mathbf{y} = \begin{bmatrix} \sigma_{r1}^2 \\ \sigma_{r2}^2 \\ \vdots \\ \sigma_{rn}^2 \end{bmatrix} \tag{13}$$

where x_i, $i = 1, \ldots, n$, is the nth distance reading. A quadratic polynomial, $\mathbf{y} = a_0\mathbf{v}_0 + a_1\mathbf{v}_1 + a_2\mathbf{v}_2$, was utilized as the fitting equation. Let $\mathbf{C}_\sigma$ be the $n \times 3$ matrix $\mathbf{C}_\sigma = [\mathbf{v}_0, \mathbf{v}_1, \mathbf{v}_2]$. The coefficients can be approximated by:

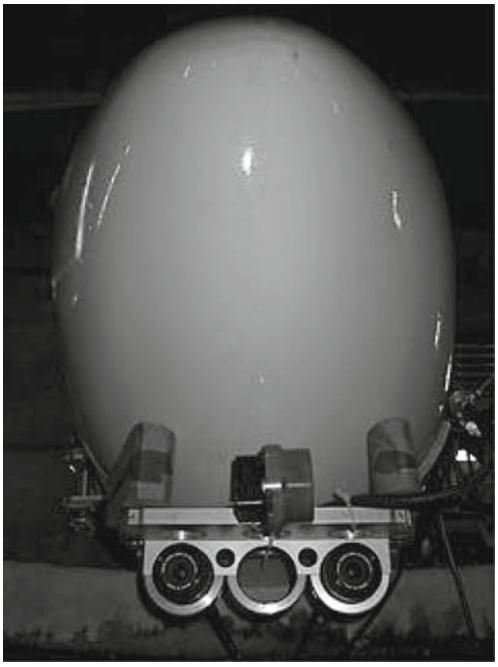

Fig. 6. The CCD cameras and ranging sonar mounted on the BAUV

$$\begin{bmatrix} a_0 \\ a_1 \\ a_2 \end{bmatrix} = (\mathbf{C}_\sigma^{\mathrm{T}} \mathbf{C}_\sigma)^{-1} \mathbf{C}_\sigma^T \mathbf{y} \tag{14}$$

The experiment was conducted in a water tank 120 m long, 8 m wide and 4 m deep. The target was set 4 m in front of the BAUV. Sonar was first used to detect the mooring cable position. When the BAUV approached the mooring cable in the visible range, the new waypoint information from the sonar measurement was combined and then updated with measurements from the CCD cameras. Figure 6 shows the CCD cameras and sonar mounted on the BAUV. Figure 7 shows images captured from the right camera when the BAUV was approaching the cable. Images were processed through thresholding

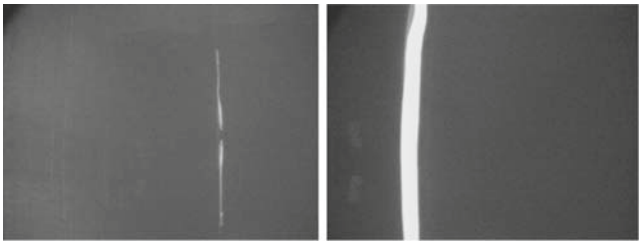

Fig. 7. Images captured by the right camera with the BAUV approaching the target at **a** $t = 10$ s and **b** $t = 80$ s

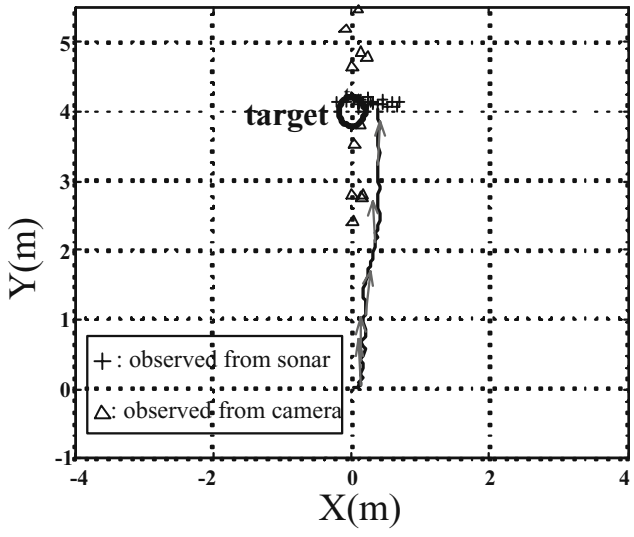

Fig. 8. The BAUV position derived from Doppler sonar, and the cable position derived from sonar and stereo images. *Lines with arrows* indicate headings at the respective BAUV positions

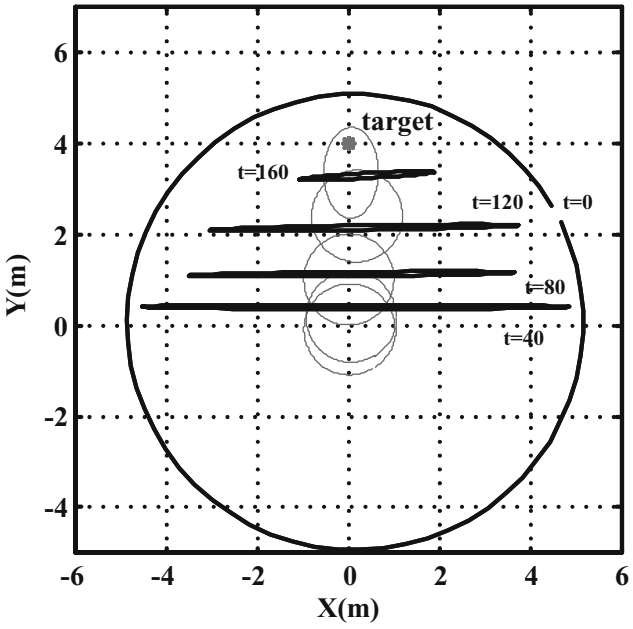

Fig. 9. Positional uncertainties of the BAUV. *Thick lines* indicate uncertainty propagation with time t derived from the ranging sonar. *Thin lines* represent uncertainty propagation derived from the CCD cameras

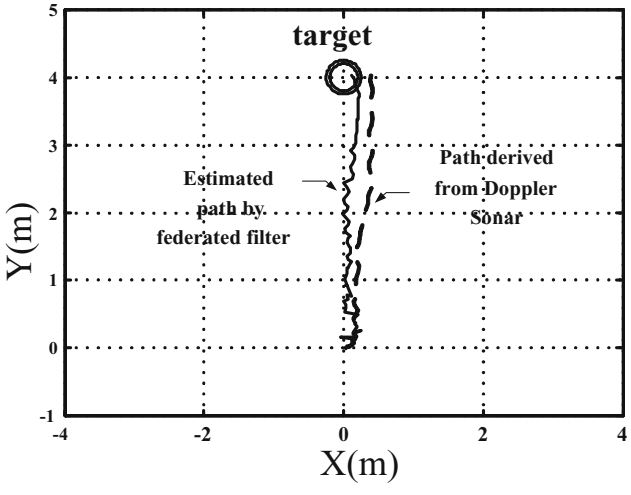

Fig. 10. Estimated path of the BAUV from the federated filter

and edge detection to acquire a value for the target distance. Figure 8 presents the positional data measured using Doppler sonar, and the cable positions estimated by the ranging sonar and CCD cameras. To combine data from the sensors, the federated filter algorithm presented in Sect. 3 was used. The federated filter estimates BAUV positions by fusing measurements from the Doppler sonar, the ranging sonar, and CCD cameras. Figure 9 shows the BAUV positional uncertainty calculated by the ranging sonar and CCD cameras, respectively. The vehicle first used ranging sonar to detect the cable position. At first, large uncertainties existed in the x and y directions. After the ranging sonar received data for the relative distance between the BAUV and the cable, the uncertainty in the y direction decreased much more than the reduction in the x direction. Finally, when the BAUV was close to the mooring cable, camera measurements were utilized to decrease the uncertainty in the x direction. The trajectory record shown in Fig. 10 indicates that the position of the BAUV was estimated accurately; the final position of the BAUV was at the mooring cable.

4 Conclusions

This work presents a control system for underwater tracking of a mooring cable using active sensing for a BAUV. A sonar and CCD cameras were employed as sensors to detect and estimate the mooring cable position. A Doppler velocity log was used as the internal

sensor to estimate BAUV location. First, the BAUV searches for a cable position that indicates the mooring station location using ranging sonar. An extended Kalman filter was developed based on the BAUV kinematics for navigation in an unknown environment with data for positional uncertainty. When the BAUV swims toward a target that is close, environmental data from ranging sonar and binocular vision is utilized to estimate the cable position. A federated filter was applied to combine estimated states and error covariances from both sensors. The positional information from the federated filter was then utilized as feedback data for the BAUV control system. Tank experimental results suggest that the BAUV can successfully locate and track an underwater mooring cable, verifying the utility of the proposed approach.

Acknowledgments. The author would like to thank the National Science Council of the Republic of China, Taiwan, for financially supporting this research under Contract No. NSC91-2611-E002-008. Students Chen HW, Wu JH, Wu CH, Chen CC, Ho YS, Chi PC, Jeong YJ, and Tsai MJ helped conduct the water tank experiments.

References

1. Howe BM, McGinnis T, Boyd ML (2007) Sensor network infrastructure: moorings, mobile platforms, and integrated acoustics. In: Proceedings of the symposium on underwater technology. IEEE, Tokyo, pp 47–51
2. Guo J, Chiu FC, Chen CC, Ho YS (2003) Determining the bodily motion of a biomimetic underwater vehicle under oscillating propulsion. In: Proceedings of the IEEE international conference on robotics and automation. IEEE, Taipei, pp 983–988
3. Guo J (2006) A waypoint-tracking controller for a biomimetic autonomous underwater vehicle. Ocean Eng 33:2369–2380
4. Miura J, Shirai Y (1997) Vision and motion planning for a mobile robot under uncertainty. Int J Robot Res 16(6): 806–825
5. Moon I, Miura J, Shirai Y (1999) On-line viewpoint and motion planning for efficient visual navigation under uncertainty. Robot Auton Syst 28:237–248
6. Davison AJ, Murray DW (2002) Simultaneous localization and map building using active vision. IEEE Trans Pattern Anal Mach Intell 24(7):865–880
7. Guo J, Tsai JF, Chiu FC, Lee YJ (2007) Optimal measurement strategies for target tracking by a biomimetic underwater vehicle. In: Proceedings of the 17th international offshore (ocean) and polar engineering conference. The International Society of Offshore and Polar Engineers, Lisbon
8. Williams SB, Newman P, Dissanayake G, Durrant-Whyte H (2001) Autonomous underwater navigation and control. Robotica 19:481–496
9. Guo J, Joeng YJ (2004) Guidance and control of a biomimetic-autonomous underwater vehicle using body-fin propulsion. J Eng Mar Environ 218:93–111
10. Carlson NA (1990) Federated square root filter for decentralized parallel processes. IEEE Trans Aerospace Elect Syst 26(3):517–525
11. Matthies LS, Shafer A (1987) Error modelling in stereo navigation. IEEE J Robot Autom 3(3):239–248
12. Benet GM, Blanes F (2005) Differentiating walls from corners using the amplitude of ultrasonic echoes. Robot Auton Syst 50:13–25